

## NUMERICAL ALGORITHM FOR SUBSTRUCTURE ON-LINE COMPUTER TESTING

Makoto KANDA<sup>1)</sup>, Nobuaki SHIRAI<sup>2)</sup> and Minoru MOTOKI<sup>3)</sup>

- 1) Department of Architecture and Architectural Engineering, College of Industrial Technology, Nihon University,  
Izumicho 1-2-1, Narashino, Chiba, Japan, 275
- 2) Department of Architecture, College of Science and Technology, Nihon University,  
Kandasurugadai 1-8, Chiyoda, Tokyo, Japan, 101
- 3) Tomoe Corporation,  
Kachidoki 4-5-17, Chuo, Tokyo, Japan, 104

### Abstract

The numerical integration-control algorithm for substructure on-line computer testing was proposed in this paper. The algorithm is able to handle three abilities which are to have weaker stability criteria, to apply the load and / or displacement control and to dissipate spurious growth of higher mode response. The validity of the algorithm was verified by means of numerical experiment of substructure on-line test on the frame structure.

### Keywords

Substructure on-line computer testing; implicit integration scheme; load control;  $\alpha$ -method.

### 1. Introduction

Recently, a new technique, which incorporated the concept of substructure analysis (Bathe, k, 1982) into the on-line computer testing (Hakuno et. al., 1969; Takanashi et al., 1974), which is referred to as "OLT", has been developed to investigate inelastic dynamic behaviors of structures. This technique is able to simulate inelastic dynamic behavior of structure by conducting quasi-static loading test on only a part of structure and is referred to as "substructure on-line computer testing (SOT) (Mahin et al., 1985; Nakashima et al., 1991)". Since the SOT has a lot of advantages, it may become a major testing technique for investigating inelastic dynamic behavior of structure. However, application of the SOT has been limited to a specific type of structures so far. This may be due to the following issues to be solved (Nakashima et al., 1991; Shing and Mahin, 1983);

- I. Stability of solution for multi-degrees of freedom system.
- II. Applicability of the displacement control technique to degrees of freedom with high stiffness.
- III. Spurious growth of higher mode responses due to experimentally generated errors.

To solve these problems and also to make the SOT practically feasible, it must be needed to develop a numerical integration-control algorithm which satisfies the following conditions;

1. A numerical integration scheme should have weaker stability criteria and it is desirable that it is unconditionally stable if possible.
2. It has capability for applying the load and/or displacement control.
3. It has ability for dissipating spurious growth of higher mode responses.

The objective of this paper is to develop a numerical integration-control algorithm which is applicable to the SOT and has an ability satisfying in the conditions.

## 2. Numerical integration -control algorithm for SOT

### 2.1 Principle of SOT

In the SOT, total structure is separated into two subassemblages. One is an experimental subassemblage whose restoring force shall be obtained by means of actual loading test. The other is an analytical subassemblage whose restoring force shall be calculated by means of mathematical model. Then, the restoring forces of two subassemblages are coupled based on the concept of substructure analysis. Generally, structural subassemblage, which has complex restoring force characteristics or may govern overall behavior of structure, is modeled as the experimental subassemblage. The remaining subassemblage of structure is modeled as the analytical subassemblage. Fig. 1 shows an example of substructure modeling for 3-span and multi-story framed structure. The outer columns in the first story were modeled as the experimental subassemblage and the remaining members were modeled as the analytical subassemblage. The restoring force vector for overall structure can be obtained by superimpose two restoring force vectors corresponding to both subassemblages. Consequently, the equation of motion for the SOT can be expressed as follows;

$$M\Delta\ddot{X} + C\Delta\dot{X} + \Delta R = \Delta F \quad (1)$$

$$\text{in which, } \Delta R = \Delta\tilde{R} + \Delta\hat{R} \quad (2)$$

where  $M$  and  $C$  indicate the mass and damping matrices,  $\Delta F$ ,  $\Delta\ddot{X}$  and  $\Delta\dot{X}$  indicate the external force, acceleration and velocity increment vectors, and  $\Delta R$ ,  $\Delta\tilde{R}$  and  $\Delta\hat{R}$  indicate the restoring force increment vectors of total structure, experimental subassemblage and analytical subassemblage.

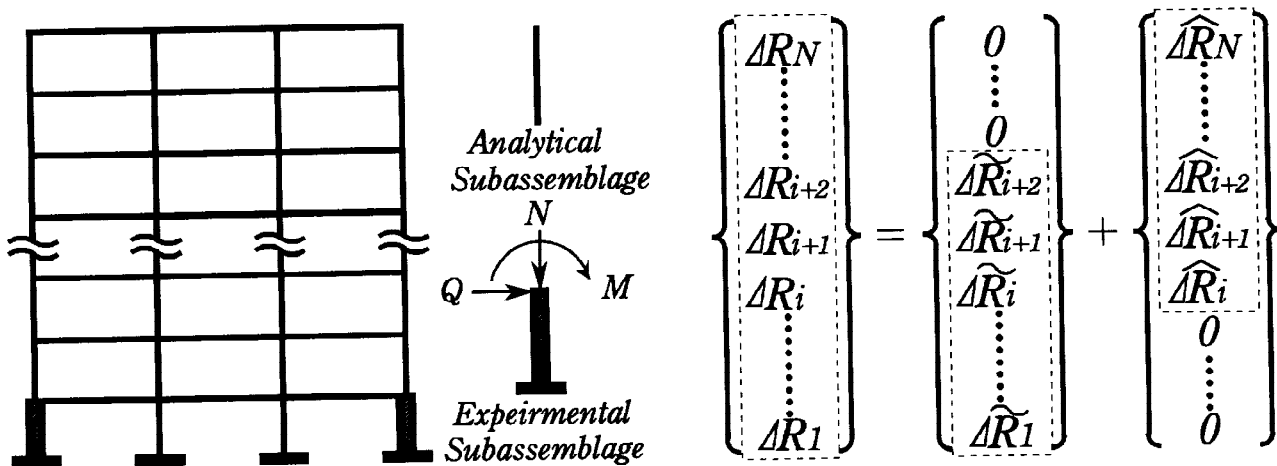


Fig. 1 Concept of SOT

### 2.2 Conditions and limitations of numerical integration-control algorithm for SOT

As stated in chapter 1, a numerical integration-control algorithm to be proposed must have the abilities being able to overcome the issues of I to III. Furthermore, since the SOT is different from the standard earthquake response analysis with respect to several aspects, there exists several limitations encountered during the

numerical integration process in the SOT.

The SOT is an efficient approach which can investigate dynamic behavior of structure with complex hysteresis properties. In fact, tangential stiffness of experimental subassemblage would vary in a complex manner. Also, it is extremely difficult to evaluate tangential stiffness for multi-degrees of freedom system during loading to be controlled according to calculated response values. Therefore, 1) it is required that an algorithm to be adopted in the SOT can simulate complex inelastic behavior of experimental subassemblage without evaluating its tangential stiffness (Shing et al., 1991). There is an iterative incremental solution procedure which obtains inelastic response of structure without evaluating its tangential stiffness. However, it may happen that controlled displacements overshoot target displacements and then they turn over their directions and approach target displacements, if the On-line computer testing incorporating an iterative solution procedure is applied to multi-degrees of freedom system. Since behavior of structure depends on experienced hysteresis path, it is not desirable that loading direction of displacements changes within a single time step. Therefore, 2) it is required that an algorithm would provide such incremental displacements that would not turn over their directions within a single time step (Shing et al., 1991; Mahin et al., 1987; Nakashima et al., 1991). In the standard earthquake response analysis, a size of integration time steps is taken to be sufficiently small to guarantee stability and accuracy of solution. In the SOT, On the other hand, displacement increment to be controlled has to be kept such a magnitude that it can be controlled accurately. It may happen that a magnitude of displacement increment becomes smaller than a controllable limit value, if a smaller size of integration time steps,  $\Delta t$ , is used. Therefore, 3) it is required that one should not make a size of time steps smaller boundlessly. An algorithm must possess the abilities of I, II and III although it is subject to the limitations of 1), 2) and 3). For example, Mahin et al. (Shing et al., 1991; Mahin et al., 1987) proposed an algorithm that the control would be executed while correcting target displacements based on the dynamic equilibrium equation within a single time step. This algorithm satisfies the condition stated in the above. When the algorithm is applied to the structure with multi-degrees of freedom as shown in Fig. 1, it may happen that the calculation speed can not follow the loading speed of actuator since the computational time increases greatly to obtain target displacements to be corrected. Finally, 4) it is recommended that an algorithm is not required to correct target displacements consecutively and a control technique similar to that of explicit integration scheme can be applicable if possible (Nakashima et al., 1991).

### 2.3 Formulation of numerical integration - control algorithm

An algorithm to be proposed is based on the implicit Newmark  $\beta$ -method which incorporated the initial stress method (Zienkiewicz, 1984) to obtain converged solution iteratively with fictitious stiffness and unbalanced forces. Therefore, the increment of restoring force vector  $\Delta R$  can be expressed as  $\Delta R = K_I X - \Delta R''$ . Where  $\Delta R''$  indicates the increment of unbalanced force vector,  $K_I$  the assumed stiffness matrix and  $\Delta X$  the increment of displacement vector. To cope with the issue of III, the  $\alpha$ -method shall be introduced into the said numerical integration algorithm. The  $\alpha$ -method is an implicit integration algorithm which guarantees unconditional stability. It can suppress spurious growth of specified higher mode responses by means of an artificially introduced damping parameter. Consequently, the equation of motion can be expressed as follow;

$$M\Delta\ddot{X}_{n+1} + (1+\alpha)C\Delta\dot{X}_{n+1} - \alpha\Delta\dot{X}_{n+1} + (1+\alpha)K_I\Delta X_{n+1} - \alpha K_I\Delta X_n - \left\{ (1+\alpha)\Delta R''_{n+1} - \alpha\Delta R''_n \right\} = (1+\alpha)\Delta F_{n+1} - \alpha\Delta F_n \quad (3)$$

where,  $\alpha$  is the auxiliary parameter, and the subscripts  $n$  and  $n+1$  indicate the step number of discretized times. Solving the equation based on the  $\alpha$ -method and applying an iterative procedure based on the initial stress method, the solution can be formulated in the form of recurrence equation as follows;

$$\Delta X_{n+1}^{(k+1)} = K_I^{*-1} \left\{ \Delta F_{n+1}^* + (1+\alpha)\Delta R_{n+1}^{n(k)} \right\} \quad (4)$$

$$\Delta\ddot{X}_{n+1} = 1/(\beta\Delta t^2) \Delta X_{n+1}^{(L)} - 1/(\beta\Delta t) \Delta\dot{X}_n - 1/(2\beta) \Delta\ddot{X}_n \quad (5)$$

$$\Delta \dot{X}_{n+1} = (\gamma / \beta \Delta t) \Delta X_{n+1}^{(L)} - (\gamma / \beta) \dot{X}_n - \{(\gamma / 2\beta) - 1\} \Delta t \ddot{X}_n \quad (6)$$

$$\Delta R_{n+1}^{(k+1)} + \Delta R_{n+1}^{u(k+1)} = K_I \Delta X_{n+1}^{(k+1)} \quad (7)$$

$$\Delta F_{n+1}^* = (1 + \alpha) \Delta F_{n+1} - \alpha \Delta F_n + M \left\{ (1 / \beta \Delta t) \dot{X}_n + 2\beta \ddot{X}_n \right\} + (1 + \alpha) C \left[ (\gamma / \beta) \dot{X}_n + \{(\gamma / 2\beta) - 1\} \Delta t \ddot{X}_n \right] + \alpha C \Delta \dot{X}_n + \alpha K_I \Delta X_n - \alpha \Delta R_n^u \quad (8)$$

$$K_I^* = (1 / \beta \Delta t^2) M + (1 + \alpha) (\gamma / \beta \Delta t) C + (1 + \alpha) K_I \quad (9)$$

$$\text{in which, } \beta = (1 - \alpha)^2 / 4, \quad \gamma = (1/2) - \alpha \quad (10)$$

$$k = 0, 1, 2, 3, \dots, L - 1, \quad \Delta R_{n+1}^{u(0)} = \emptyset, \quad \Delta X_{n+1} = \Delta X_{n+1}^{(L)} \quad (11)$$

where,  $\beta$  and  $\gamma$  are the auxiliary parameters of  $\alpha$ -method, the superscripts  $k$  and  $k+1$  are the number of iterations, and  $L$  indicates the final number of iterations in a certain step. There are cases that the limitations of 2) and 3) stated in section 2.2 may not be satisfied when an iterative calculation is executed several times. However, convergence of the proposed iteration procedure is satisfactory (Kanda and Shirai et al., 1995) and accurate solution can be obtained even if a number of iteration is only one. To cope with the limitations of 2) and 3), a number of iteration shall be only one and thus a number of corresponding control to gain a target value shall be only one. Fig. 2 shows the flowchart of proposed numerical integration algorithm.

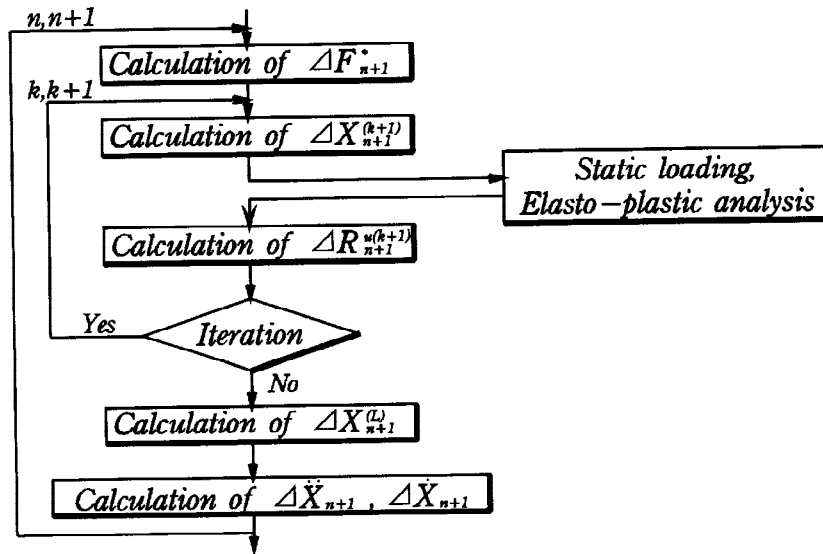


Fig. 2 Proposed Numerical Integration Algorithm

Furthermore, a control algorithm shall be constructed based on the numerical integration algorithm to solve the issue of II. In the SOT or OLT that the explicit numerical integration algorithm is utilized, it is common that response values are estimated using feedback values of experimentally measured restoring forces. The proposed algorithm is similar to the explicit algorithm in a sense that response values are estimated using unbalanced forces evaluated on the basis of experimentally measured feedback values. It is a common practice to utilize the displacement control technique in the SOT or OLT because it is easy to combine such control technique with the numerical integration algorithm. However, it is also possible to utilize the load control technique if an algorithm can be formulated so as to be compatible with such load control technique. Taking advantage of capability that the proposed algorithm can estimate response values if unbalanced forces can be evaluated using feedback values of experimentally measured restoring forces, the load control technique shall be combined with the proposed integration algorithm. Fig. 3 shows the proposed control algorithm during the process from first obtaining response displacements  $\Delta X_{n+1}^{(k+1)}$  until obtaining unbalanced forces  $R_{n+1}^{u(k+1)}$ . In this algorithm, at first it is required to obtain the target restoring force of experimental subassemblage  $\tilde{R}_{n+1}^t$  based on the following equation.

$$\tilde{R}'_{n+1} = \tilde{K}_I X'_{n+1} - \tilde{R}''_{n+1} \quad (12)$$

$$\text{in which, } X'_{n+1} = X^{(k+1)}_{n+1} \quad (13)$$

where,  $\tilde{K}_I$  indicates the assumed stiffness matrix of experimental subassemblage and  $\tilde{R}''_{n+1}$  indicates the unbalanced force vector of experimental subassemblage. The unbalanced force vectors for the experimental and analytical subassemblages are evaluated independently. Then, the unbalanced force vector of total structure is calculated by superimposing those unbalanced force vectors.

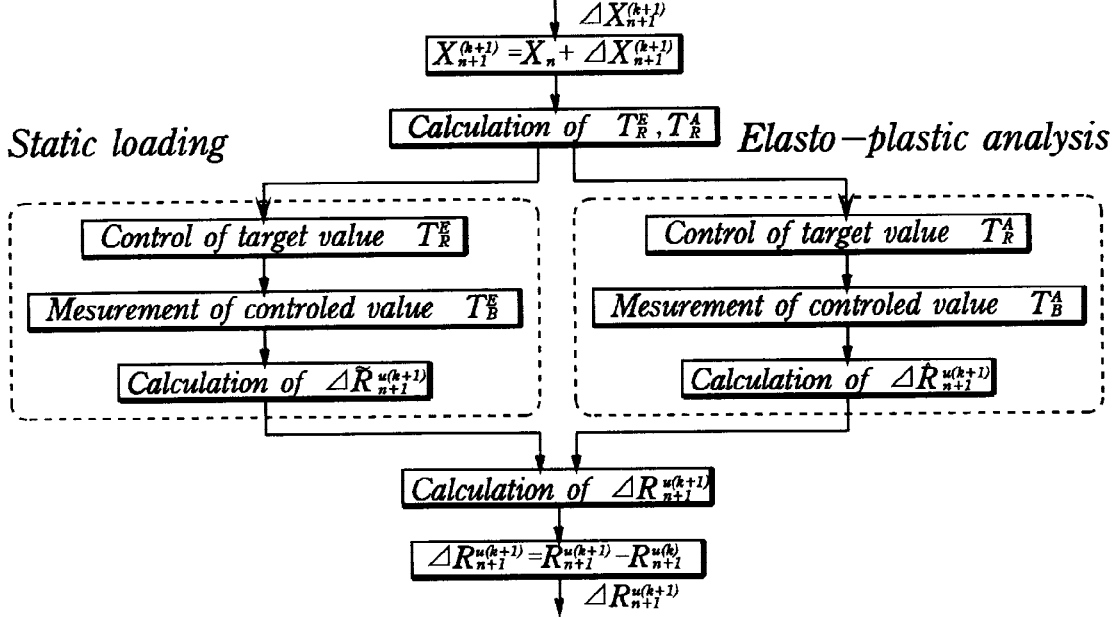


Fig. 3 Proposed Control Algorithm

The matrices of  $I_L$ ,  $I_D$ ,  $J^E$  and  $J^A$  shall be introduced to evaluate target values to be controlled and unbalanced forces for both subassemblages systematically. Where  $I_D$  and  $I_L$  indicate the matrices for selecting either the load control or the displacement control,  $J^E$  and  $J^A$  indicate the matrices that transform the target vector of total system to the decomposed target vectors of each subassemblage. The target vectors for both subassemblages,  $I$  and  $J$ , can be obtained in terms of  $T_R^E$  and  $T_R^A$  as follows;

$$T_R^E = I_L J^E \tilde{R}'_{n+1} + I_D J^E X'_{n+1} \quad (14)$$

$$T_R^A = J^A X'_{n+1} \quad (15)$$

$$\text{in which, } I = I_L + I_D \quad (16)$$

As is seen from Eq. (14), each element in  $T_E^R$  becomes the target value of load when the corresponding degree of freedom is controlled by the loading. Also each element in  $T_E^R$  becomes the target value of displacement when the corresponding degree of freedom is controlled by the displacement. Similarly, each element in the feedback vector  $T_B^E$  becomes the measured value of displacement when the corresponding degree of freedom is controlled by the loading. On the other hand, each element in  $T_B^E$  becomes the measured value of load when the corresponding degree of freedom is controlled by the displacement. Note that  $I$  indicates the unit matrix. Consequently, the unbalanced force vectors for both subassemblages can be obtained in terms of the feedback vectors,  $T_B^E$  and  $T_R^E$ , as follows;

$$\tilde{R}''_{n+1} = \tilde{K}_I J^{E'} (I_L T_B^E + I_D T_R^E) - J^{E'} (I_L T_R^E + I_D T_B^E) \quad (17)$$

$$\hat{R}_{n+1}^{u(k+1)} = \hat{K}_I J^{A'} T_R^A - J^{A'} T_B^A \quad (18)$$

where,  $\hat{R}_{n+1}^{u(k+1)}$  indicates the unbalanced force vector for the analytical subassemblage, and  $J^{A'}$  and  $J^{E'}$  indicate the transpose matrices of  $J^A$  and  $J^E$ , respectively. Finally, the unbalanced force vector for total system can be obtained by the following equation;

$$R_{n+1}^{u(k+1)} = \tilde{R}_{n+1}^{u(k+1)} + \hat{R}_{n+1}^{u(k+1)} \quad (19)$$

In the next place, the matrices of  $J^E$ ,  $J^A$ ,  $I_L$  and  $I_D$  shall be described in detail. Fig. 4 shows the shear spring-mass model with four degrees of freedom. A number of row in  $J^E$  and  $J^A$  is equal to that of degrees of freedom for each subassemblage and a number of column in  $J^E$  or  $J^A$  is equal to that of degrees of freedom for total system. If the structural part including the masses of 1 and 2 is modeled as the experimental subassemblage and the other part including the masses of 2, 3 and 4 is modeled as the analytical subassemblage, the mass of 2 will be shared by both subassemblages. In this case,  $J^E$  and  $J^A$  can be expressed as indicated in Fig. 4 Note that  $J^E$  and  $J^A$  are the square matrices and a number of row and column composing those matrices is equal to the degree of freedom for the experimental subassemblage. In case that the mass of 1 is controlled by the load and on the other hand the mass of 2 is controlled by the displacement,  $I_L$  and  $I_D$  can be expressed as indicated in Fig. 4 Furthermore, it is possible to switch from the load control to the displacement control or vice versa only by exchanging the corresponding elements in  $I_L$  and  $I_D$ .

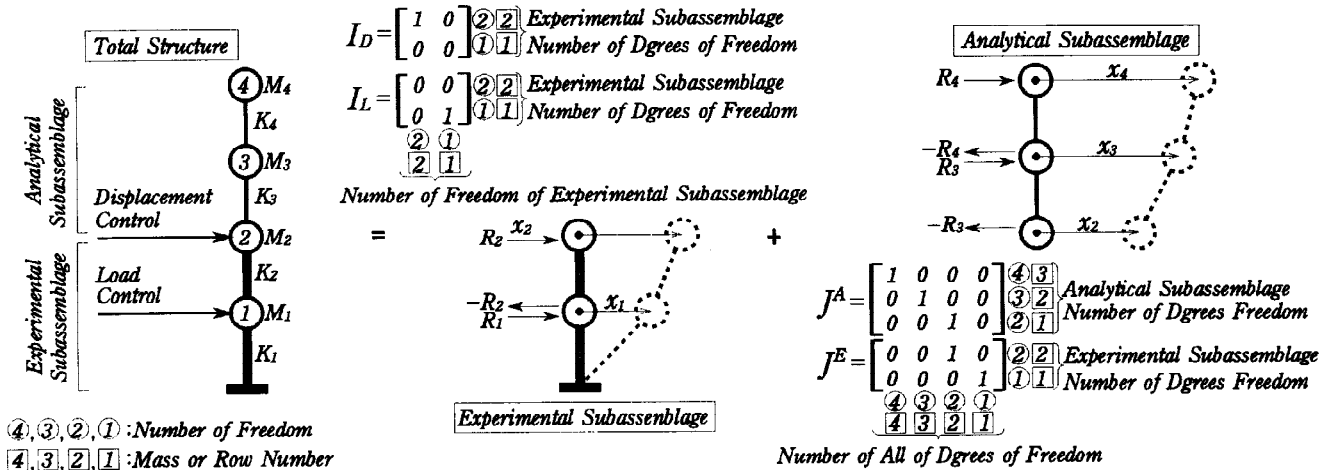


Fig. 4 Example of  $I$  and  $J$  for Shear Spring-Mass Model with Four Degrees of Freedom System

### 3. Verification of numerical integration-control algorithm by means of numeral experiment

In this chapter, validity of the proposed algorithm is verified by conducting the numerical SOT on the framed model as sown in Fig. 5 The parameters to be used are listed in Table. 1. The analysis model is a single-span 3-story framed structure with braces at second and third stories. The columns at first story, which are reinforced concrete members, were selected as the experimental subassemblage. Thus, the horizontal, rotational and axial degrees of freedom in those columns have to be controlled. Note that these columns have extremely high axial stiffnesses. The input excitation used is the N-S component of EL-CENTRO earthquake accelerations. The restoring force of reinforced concrete columns; that is, the experimental subassemblage, shall be evaluated by applying the fiber method (Kanda, Shirai et al., 1989) instead of actual loading test. On the other hand, the remaining part of structure was modeled as the analytical subassemblage and was assumed to behave within an elastic range. Furthermore, for comparison, it is assumed that the response to be evaluated by the explicit Newmark- $\beta$  method with  $\varpi, \Delta t = 1.5$ , can be regarded as the exact solution. Thus, the exact solution is compared with the response obtained by the proposed algorithm with  $\varpi, \Delta t = 3.0$ . In case 1, it will be studied whether the proposed algorithm can suppress propagation of experimental errors and can provide stable and

accurate solution even with relatively large  $\Delta t$ . The input error introduced is the undershoot displacement of  $20\mu m$  which corresponds to the amount measured by the actual loading test. In case 2, it will be studied whether the proposed algorithm makes feasible to conduct the numerical experiment while selecting the advantageous control technique either the displacement control or the load control.

Table .1 Experimental Parameters

case	Numerical Integration	Damping Factor	Control Method			Remark
			Horizontal (Q)	Rotation (M)	Axial (N)	
1	Explicit Newmark- $\beta$ Method	$h_1 = 0.0$	Displacement Control	Displacement Control	Displacement Control	Exact Solution
	Proposed Algorithm ( $\alpha = 0$ )					Undershoot $20 \mu m$
	Proposed Algorithm ( $\alpha = -1/3$ )					Undershoot $20 \mu m$
2	Explicit Newmark- $\beta$ Method	Rayleigh $h_1 = 0.02$	Displacement Control	Displacement Control	Displacement Control	Exact Solution
	Proposed Algorithm ( $\alpha = 0$ )					---
	Proposed Algorithm ( $\alpha = 0$ )					---

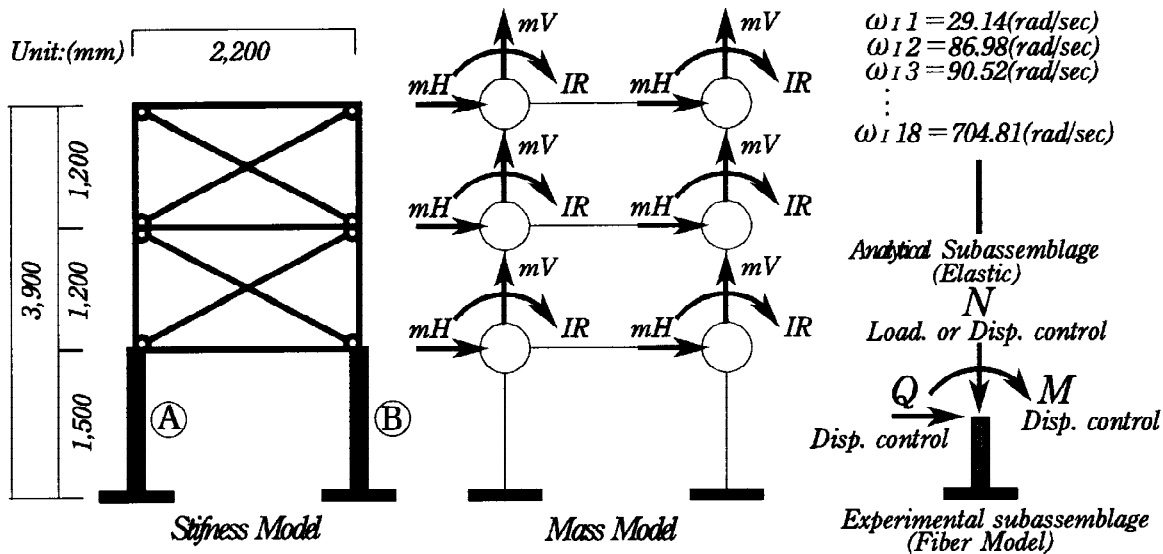


Fig. 5 Analytical Model

Fig. 6 shows the time history of responses for A in the experimental subassemblage (case 1). When  $\alpha = 0$ , spurious higher mode responses due to the undershoot error were observed. On the other hand, when  $\alpha = -1/3$ , the stable and accurate solution was obtained although the experimental error was introduced. This may be due to the reason that the numerical damping parameter suppressed superiors higher mode responses.

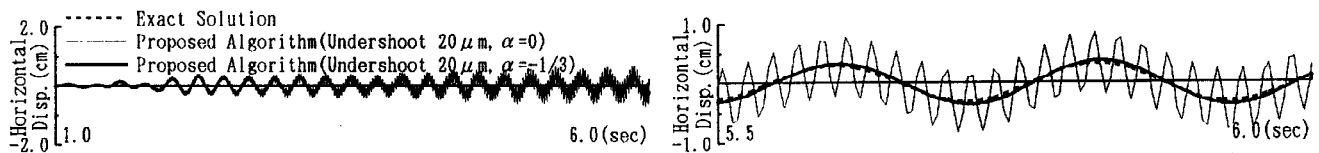


Fig. 6 Times History (Horizontal Displacement)

Fig. 7 shows the time histories of responses for A in the experimental subassemblage (case 2). Fig. 7(a) shows the result obtained by applying the displacement control to the axial direction and Fig. 7(b) shows the result obtained by applying the load control to the axial direction. As stated in the above, the load control is desirable

when controlling degree of freedom associated with such high axial stiffness as column because incremental displacement to be controlled may become smaller than the allowable limit value which can be controlled by the actuator accurately. The response result obtained by the load control agrees well with the exact solution. Therefore, it was confirmed that reliable SOT could be done by the loading and/or displacement controls if the proposed algorithm would be applied.

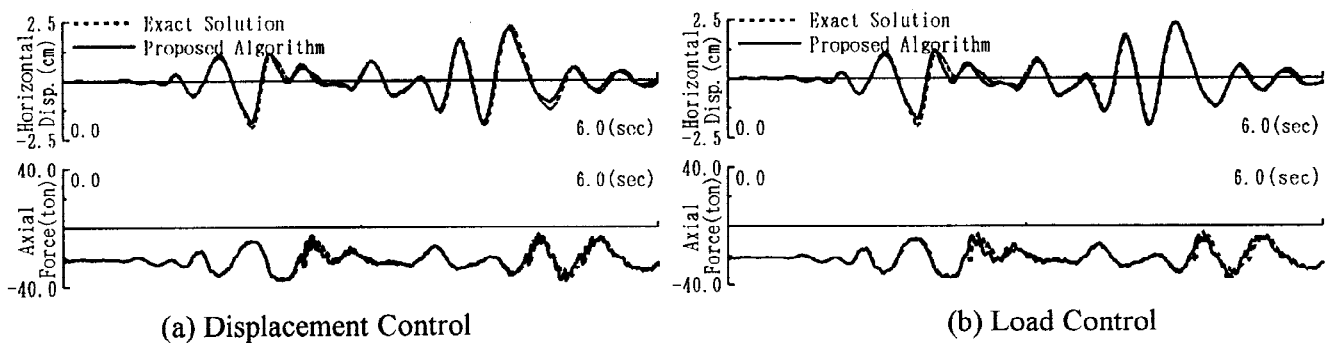


Fig. 7 Time Histories of Horizontal Displacement and Axial Force

#### 4. Conclusion

The numerical integration-control algorithm, which can be applicable to the SOT, was proposed and the numerical experiment was conducted by applying the proposed algorithm. The following conclusions were obtained;

- 1) The proposed algorithm can provide stable and accurate solution even for high frequency modes as well as low frequency modes.
- 2) The proposed algorithm can suppress the growth of spurious higher mode responses generated by experimental errors without distorting lower mode responses.
- 3) The proposed algorithm can apply the load and/or displacement controls.

#### References

- Bathe, K (1982). *Finite Element Procedures in Engineering Analysis*. Prentice-Hall, INC., Englewood Cliffs, New Jersey.
- Dermutzakeis, S. N and Mahin, S. A. (1985) *Development of Substructuring Techniques for On-line Computer Controlled Seismic Performance Testing*. EERC Report, No. UCB/EERC-85/04.
- Kanda, M., Adachi, H., Shirai, N., and Nakanishi, M. (1995). *Implicit Integration Scheme Based on Initial Stress Method for Substructure On-line Testing*, *J. Struct. Constr. Eng., AIJ*, No. 473, pp. 75-84
- Kanda, M., Shirai, N., Adachi, H., and Sato, T. (1989). *Analytical Study on Elasto-Plastic Hysteretic Behavior of Reinforced Concrete members*, *Transactions of the Japan Concrete Institute*.
- Hakuno, M., Shidawara, M., and Hara, T. (1969). *Dynamic Destructive Test of a Cantilever Beam Controlled by an Analog-Computer*, *J. Civil Engineering*, Vol. 171.
- Nakashima, M., Ishida, M., and Ando, K. (1990). *Integration Techniques for Substructure Pseudo Dynamic Test*. *Journal of Struct. Constr. Engng. AIJ*, No. 417, pp. 107-117.
- Shing, P. B. and Mahin, S. A. (1983). *Experimental Error Propagation in Pseudo Dynamic Testing*. EERC Report No. UCB/EERC-83/12.
- Shing, P. B., Vannan, M. T., and Carter, E. (1991). *Implicit Time Integration for Pseudo Dynamic Testing*. *Earthquake Engineering and Structural Dynamic*, Vol. 20, pp. 551-576.
- Takanashi, K., Udagawa, K., Seki, M., Okada, T., and Tanaka, H. (1974). *Non-Linear Earthquake Response Analysis of Structures by a Computer-Actuator On-line System*. *Terms of AIJ*, No. 229, pp. 77-83.
- Thewalt, C. R., and Mahin, S. A. (1987). *Hybrid Solution Techniques for Generalized Pseudo Dynamic Testing*. EERC. Report No. UCB/EERC 87/09.
- O. C. Zienkiewicz (1971). *The Finite Element Method in Engineering Science*, McGraw-Hill.